Electronic Supplementary Material (ESI) for Chemical Science.

Taming the Stilbene Radical Anion

Grégoire Sieg,[1] Igor Müller[1], Kilian Weißer[2] and C. Gunnar Werncke[1]

[1] Chemistry Department, Philipps-University, Hans-Meerwein-Str. 4, 35043 Marburg, Germany. E-mail: gunnar.werncke@chemie.uni-marburg.de.

[2] Institute for Chemistry, Humboldt-University Berlin, Brook-Taylor-Str. 2, 12489 Berlin, Germany.

Table of Content

1. General considerations

All manipulations were carried out in a glovebox under a dry argon atmosphere, unless indicated otherwise. Used solvents were dried by continuous distillation over sodium metal for several days, degassed via three freeze-pump cycles and stored over molecular sieves 4 Å. Deuterated solvents were used as received, degassed via three freeze-pump cycles and stored over molecular sieves 4 Å. The ^{1}H-NMR spectra were recorded on a BRUKER AV 300 and BRUKER HD 500 NMR spectrometer (Bruker Corporation, Billerica, MA, USA). Chemical shifts are reported in ppm relative to the residual proton signals of the solvent. $w_{1/2}$ is the line width of a signal at half its maximum intensity. Integrals of the broad signals of the hmds units were obtained directly or by peak fitting (in case of overlapping signals) using the MestreNova software package (Mestrelab, Santiago de Compostela, Spain). IR measurements were conducted on a Bruker Alpha ATR-IR spectrometer (Bruker Corporation, Billerica, MA, USA). Elemental analyses were performed by the “in-house” service of the Chemistry Department of the Philipps University Marburg, Germany using a CHN(S) analyzer vario MICRO Cube (Elementar Analysensysteme GmbH, Langenselbold, Germany). UV/Vis-spectra were recorded on an AnalytikJena Specord S600 diode array spectrometer (AnalytikJena, Jena, Germany). EPR spectra were recorded on a BRUKER Magnettech ESR5000 spectrometer. EPR simulations were performed using the program EasySpin.[1]

Mössbauer spectra were recorded on a SeeCo MS6 spectrometer. The spectrometer comprises the following instruments: A Janis CCS-850 cryostat, including a CTI-Cryogenics closed cycle 10K refrigerator and a CTI-Cryogenics 8200 helium compressor. Temperature was controlled by a LakeShore 335 temperature controller. Spectra were recorded using a LND45431 Kr gas proportional counter with beryllium window connected to the SeeCo W204 gamma-ray spectrometer. The W204 includes high voltage supply, a 10 bit and 5 µs ADC and two single channel analyzers. Motor control and recording of spectra was taken care of by the W304 resonant gamma-ray spectrometer. For the reported spectra a Rivertec MCo7.114 source (57Co in Rh matrix) with an activity of about 1 GBq was used. Spectra were recorded in plastic sample holders with about 30 mg of sample at 13 K and data was accumulated for about 48 hours each. Mößbauer data was processed and simulated using the WMOSS4 program ver. F (www.wmoss.org). Isomeric shifts are referenced to alpha-iron at room temperature.

(*Z*)-Stilbene, (*Z*)-propenylbenzene and (*Z*)-3-hexene were purchased from commercial sources. $[Fe(N(SiMe_3)_2)_2]$, $[Co(N(SiMe_3)_2)_2]$, $K\{18c6\}[M(N(SiMe_3)_2)_2]$ (Fe and Co), were prepared according to literature procedures.[2–4] KC_8 was prepared by mixing respective amounts of graphite (previously dried in vacuo using a heat gun) with freshly cut potassium metal. The mixture was heated in vacuo via heat gun until all potassium metal had reacted.

2. Synthesis and Analysis

2.1. Synthesis of $[K\{18c6\}]_2[C_{14}H_{12}][Fe^{II}(N(SiMe_3)_2)_3]$ (1)

$[K\{18c6\}][Fe(N(SiMe_3)_2)_3]$ (297 mg, 0.35 mmol, 1.00 eq.), 18c6 (93 mg, 0.35 mmol, 1.00 eq.) and KC_8 (50 mg, 0.37 mmol, 1.05 eq.) were suspended in 2 mL of Et_2O. (*Z*)-stilbene (64 mg, 0.35 mmol, 1.00 eq.) was added. The mixture was filtered after a few minutes and the resulting dark brown solution was layered with 2 mL of *n*-pentane and stored at –40°C to afford **1**•(18c6)($[K\{18c6\}][Fe(N(SiMe_3)_2)_3]$) as dark brown-yellow single crystals (260 mg, 0.19 mmol, 61%).

^{1}H-NMR ([D8]THF, 300 MHz, 300 K, ppm): 3.47 (s, 48H, O-CH_2), –2.54 (br, 54H, $SiMe_3$)

Notes:

Due to paramagnetically induced signal broadening, the proton signals for the stilbene radical anion could not be detected.

The signal integral for $[K\{18c6\}]^+$ is determined by subtracting the amount of solvent residue signal from the overlapping signals at 3.47 ppm.

Elemental analysis: calculated ($C_{98}H_{216}Fe_2K_3N_6O_{24}Si_{12}$) C 48.46 H 8.96 N 3.46; experimental C 48.99 H 8.42 N 3.91
IR (ATR, cm^{-1}): 2942 (w), 2887 (w), 1560 (w), 1472 (w), 1453 (w), 1352 (w), 1280 (w), 1233 (m), 1105 (s), 976 (s), 864 (m), 823 (s), 780 (m), 749 (m), 7088 (w), 658 (m), 609 (w), 529 (w), 502 (w).

Crystals, suitable for X-ray diffraction analysis were obtained by layering a solution of **1** in Et_2O with *n*-pentane at –40 °C.

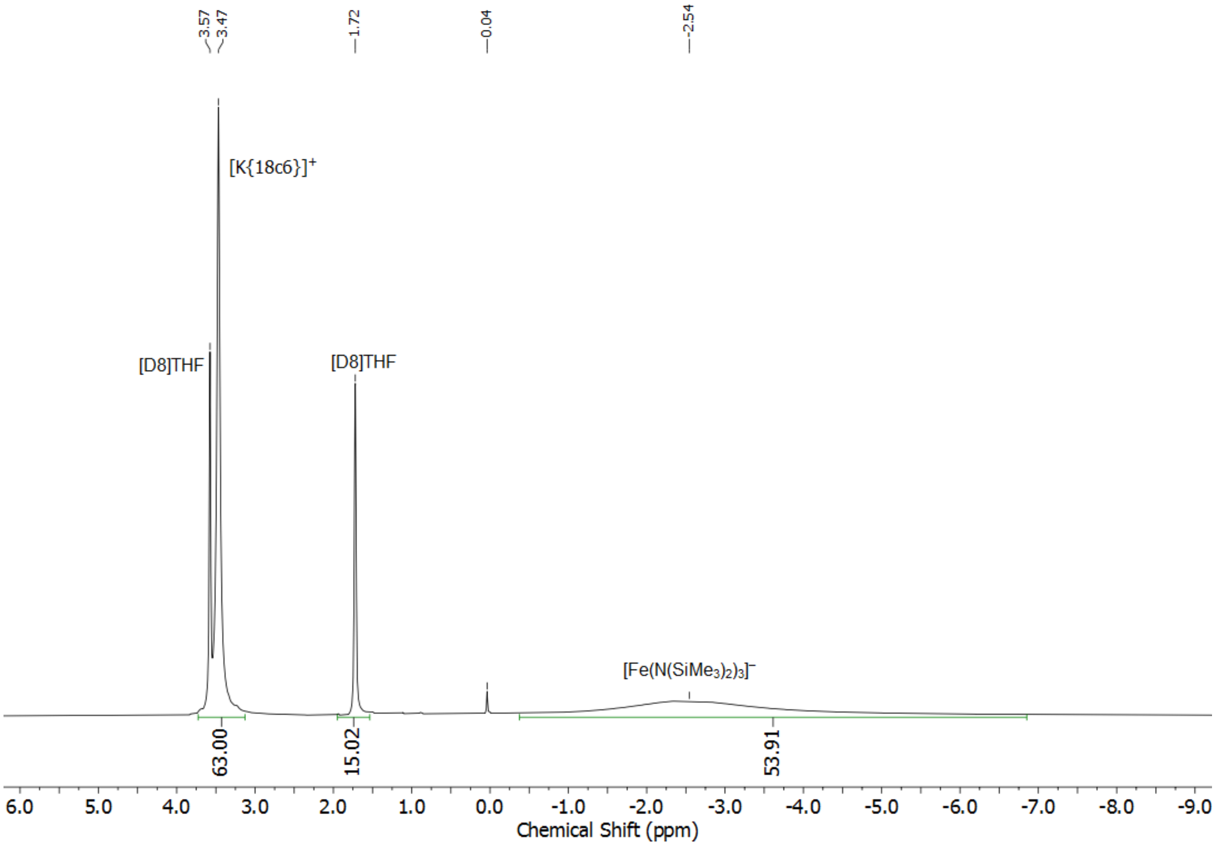

Figure S1. ^{1}H NMR spectrum of **1** in [D8]THF at 300 K, 300 MHz.

2.2. Synthesis of $[K\{18c6\}]_2[Ph_2CO][Fe^{II}(N(SiMe_3)_2)_3]$ (2)

$[K\{18c6\}][Fe(N(SiMe_3)_2)_3]$ (50 mg, 0.08 mmol, 1.00 eq.), 18c6 (21 mg, 0.08 mmol, 1.00 eq.) and KC_8 (12 mg, 0.09 mmol, 1.12 eq.) were suspended in 2 mL of Et_2O. Benzophenone (16 mg, 0.08 mmol, 1.00 eq.) was added. The mixture was filtered after a few minutes, the resulting dark blue solution layered with 2 mL of *n*-pentane and stored at -40°C to afford **2** as blue single crystals (56 mg, 0.04 mmol, 52%).

Alternative Synthesis:

1•(18c6)($[K\{18c6\}][Fe(N(SiMe_3)_2)_3]$) (63 mg, 0.026 mmol, 1.00 eq.) and benzophenone (5 mg, 0.026 mmol, 1.00 eq.) were dissolved in 2 mL of Et_2O. The solution immediately turned into deep blue. It was layered with 2 ml of *n*-pentane, stored at –40°C to afford a mixture of **2** and *E*-stilbene as crystalline solid.

^{1}H-NMR ([D8]THF, 300 MHz, 300 K, ppm): 3.45 (s, 48H, O-CH_2), –2.42 (br, 54H, $SiMe_3$)

Notes:

Due to paramagnetically induced signal broadening, the proton signals for the ketyl radical anion could not be detected.

Elemental analysis: calculated ($C_{55}H_{112}FeK_2N_3O_{13}Si_6$) C 49.82 H 8.51 N 3.17; experimental C 49.37 H 8.83 N 3.45

IR (ATR, cm^{-1}): 2942 (w), 2885 (m), 1602 (vw), 1579 (vw), 1554 (vw), 1451 (w), 1389 (vw), 1352 (m), 1284 (vw), 1233 (m), 1105 (s), 978 (s), 864 (s), 823 (s), 778 (m), 749 (m), 706 (m), 658 (m), 609 (w), 529 (vw)

Crystals, suitable for X-ray diffraction analysis were obtained by layering a solution of **2** in Et_2O with *n*-pentane at –40 °C.

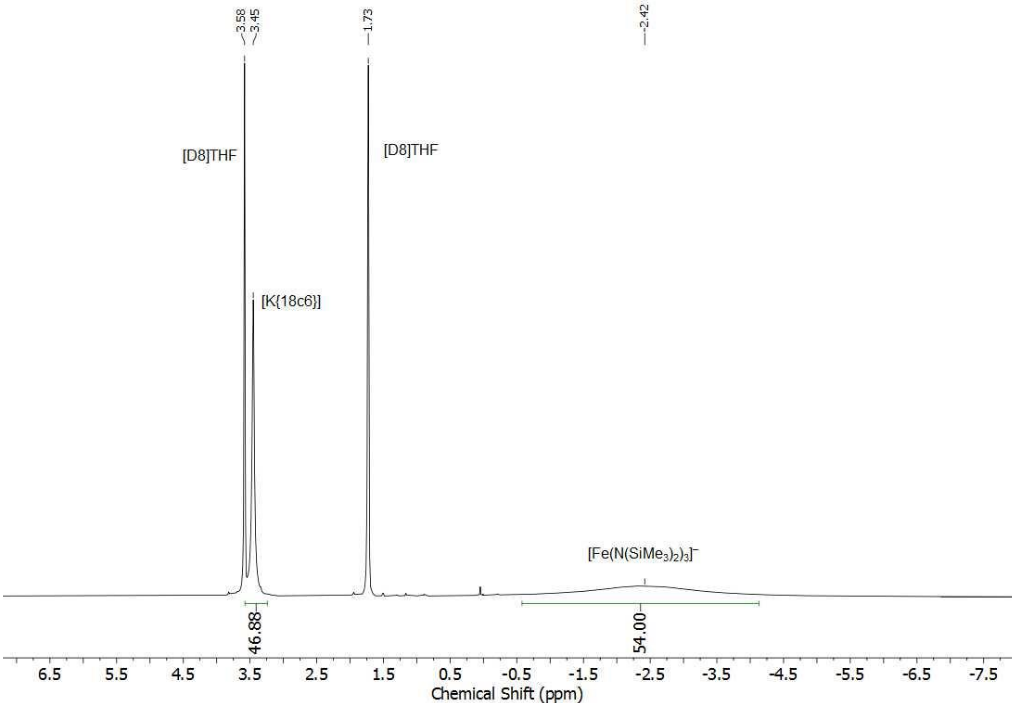

Figure S2. ^{1}H NMR spectrum of **2** in [D8]THF at 300 K, 300 MHz.

2.3. Synthesis of [K{18c6}][Fe(N(SiMe$_3$)$_2$)$_2$((*E*)-stilbene)] (3)

[K(18c6)][Fe((N(SiMe$_3$)$_2$)$_2$] (150 mg, 0.22 mmol. 1.00 eq.) and (*Z*)-stilbene (40 mg, 0.22 mmol, 1.00 eq.) were dissolved in 2 mL of Et$_2$O. After a few minutes the resulting red solution was filtered, layered with 2 mL of *n*-pentane and stored at –30 °C. The resulting red solid was filtered off and dried under vacuum to afford **3** (102 mg, 0.12 mmol, 54%).

^{1}H-NMR ([D8]THF, 300 MHz, 300 K, ppm): 92.69 (br, 1H), 91.24 (br, 0.5H), 1.94 (48H, O-CH$_2$), –6.01 (br, 36H, -SiMe$_3$), –25.29 (br, 3H).

Elemental analysis: calculated ($C_{42}H_{80}FeKN_2O_7Si_4$; **3** + Et$_2$O) C 54.10 H 8.65 N 3.00; experimental C 54.03 H 8.23 N 3.05

IR (ATR, cm^{-1}): 2940 (w), 2885 (w), 1587 (w), 1486 (w), 1470 (w), 1350 (w), 1282 (w), 1233 (m), 1173 (w), 1103 (s), 980 (s), 961 (s), 885 (m), 866 (m), 821 (s), 776 (m), 749 (m), 702 (m), 691 (m), 661 (m), 611 (m), 520 (w).

Crystals, suitable for X-ray diffraction analysis were obtained by layering a solution of **3** in Et$_2$O with *n*-pentane at –40 °C.

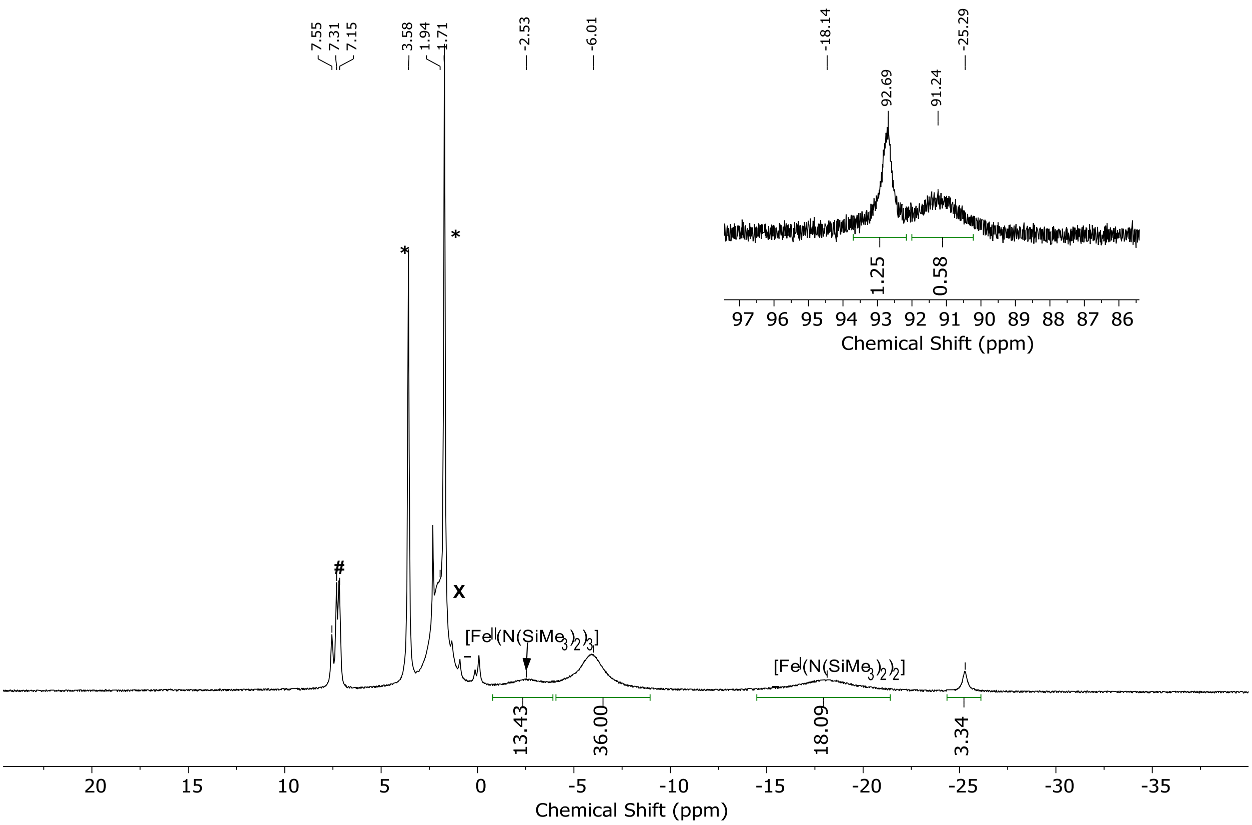

Figure S3. ^{1}H NMR spectrum of **3** in [D8]THF at 300 K, 300 MHz. *: [D8]THF, #: *E*-stilbene, X: [K{18c6}]+[D8]THF

2.4. Synthesis of $[K\{18c6\}]_2[Fe(N(SiMe_3)_2)_2((Z)\text{-ß-methylstyrene})]$ (4)

$[K(18c6)][Fe((N(SiMe_3)_2)_2]$ (68.0 mg, 0.10 mmol, 1.00 eq.) and (*Z*)-ß-methylstyrene (11.8 mg, 0.10 mmol, 1.00 eq.) were dissolved in 3 mL of Et_2O. After several hours, the reaction solution turned from green-yellow to brown. The solution was layered with 2 mL of *n*-pentane and stored at –40°C. The resulting red solid was filtered off and dried under vacuum to afford a mixture of **4** and $[K(18c6)][Fe((N(SiMe_3)_2)_2]$.

^{1}H-NMR ([D8]THF, 300 MHz, 300 K, ppm): –0.35 (br, O-CH_2, 36 H), –5.36 (br, -$SiMe_3$, 4.4 H), –18.36 (br, -$SiMe_3$, 36 H)

Crystals, suitable for X-ray diffraction analysis were obtained by layering a solution of **4** in Et_2O with *n*-pentane at –40 °C.

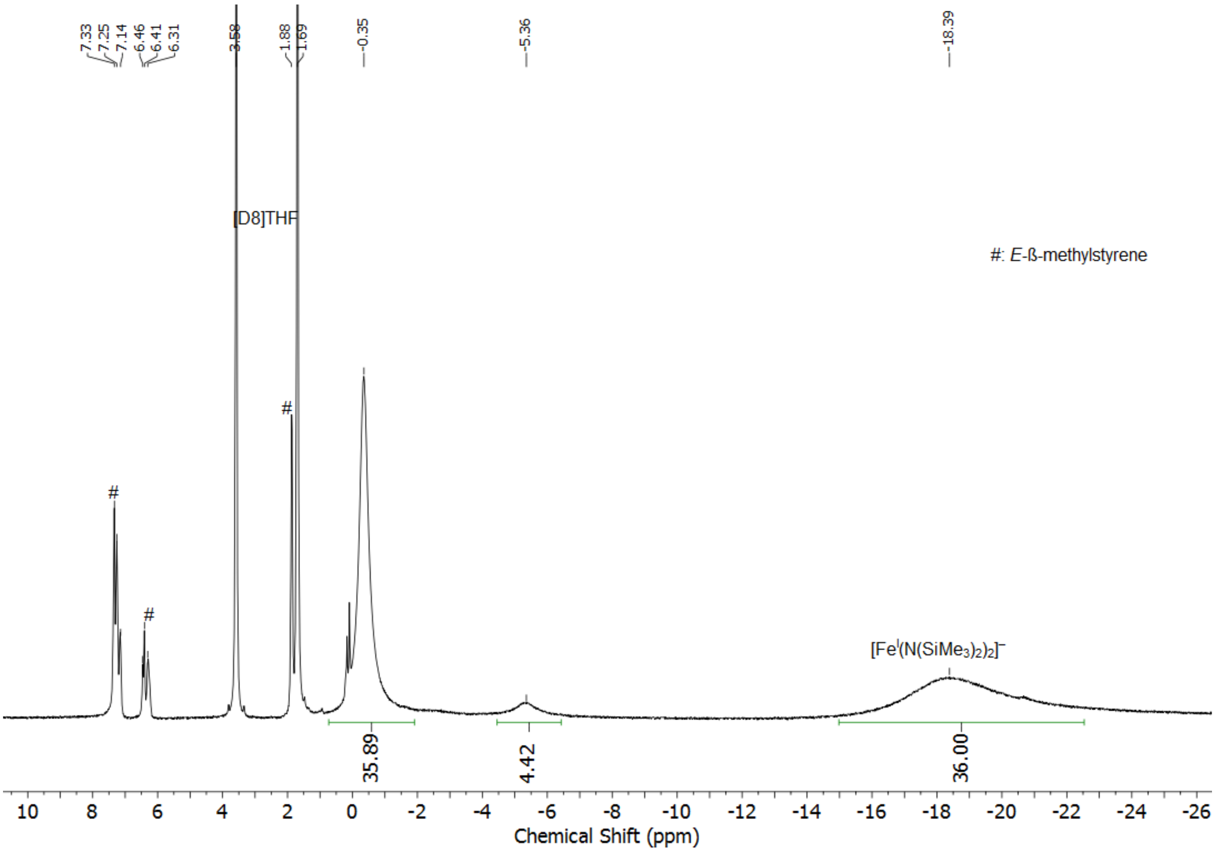

Figure S4. ^{1}H NMR spectrum of **4** in [D8]THF at 300 K, 300 MHz. #: *E*-ß-methylstyrene.

2.5. Reaction of 1 with *E*-stilbene (1 equivalent)

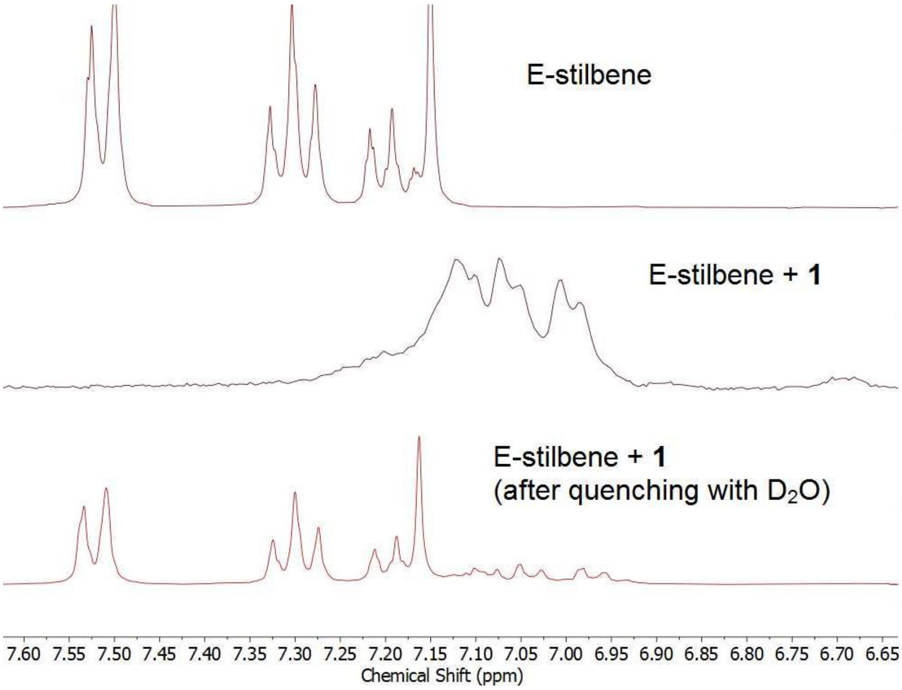

Figure S5. Top: ^{1}H NMR spectrum of *E*-stilbene. Middle: ^{1}H-NMR spectrum of *E*-stilbene with one equivalent of **1**. Bottom: ^{1}H-NMR spectrum of *E*-stilbene and one equivalent of **1** after quenching with D_2O. All spectra in [D8]THF at 300 K, 300 MHz in the range of 6.65 to 7.60 ppm.

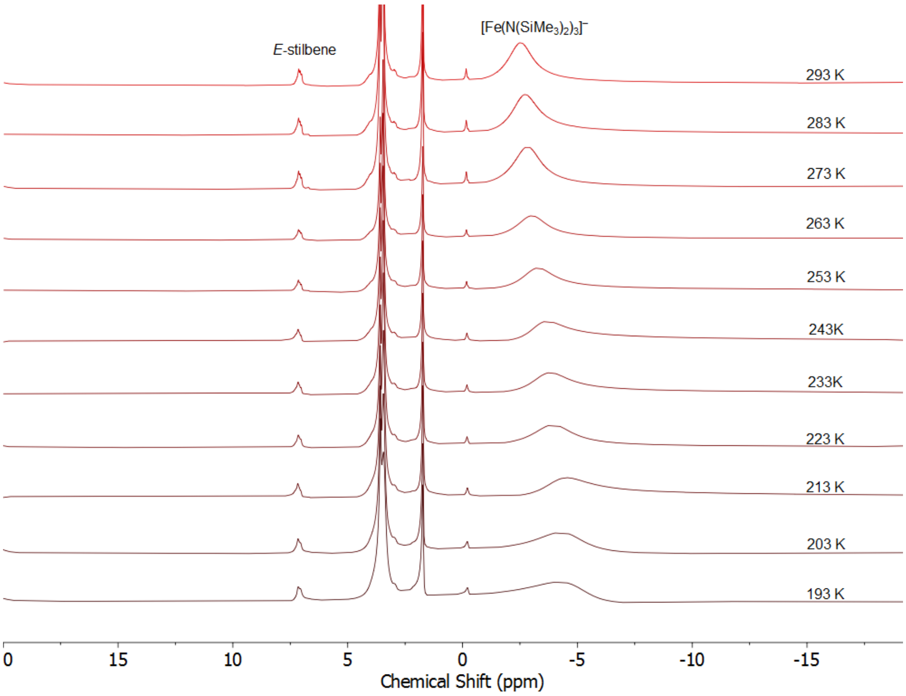

Figure S6. Temperature variable ^{1}H-NMR spectra of **1** with one equivalent of *E*-stilbene from 193 K to 293 K in [D8]THF, 500 MHz.

2.6. Reaction of 1 with *E*-stilbene (1, 5 and 10 equivalents)

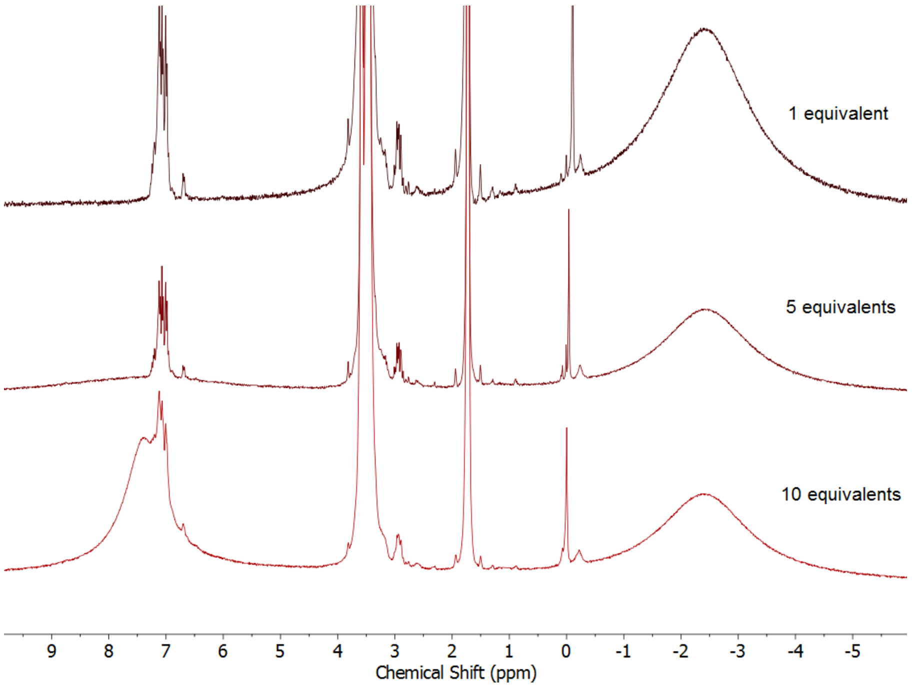

Figure S7. ^{1}H-NMR spectra of the mixture of **1** with *E*-stilbene: 1 equivalent (top), 5 equivalents (middle), 10 equivalents (bottom). All spectra in [D8]THF at 300 K, 300 MHz.

2.7. Reaction of 1 with [Co^{II}(N(SiMe$_3$)$_2$)$_2$]

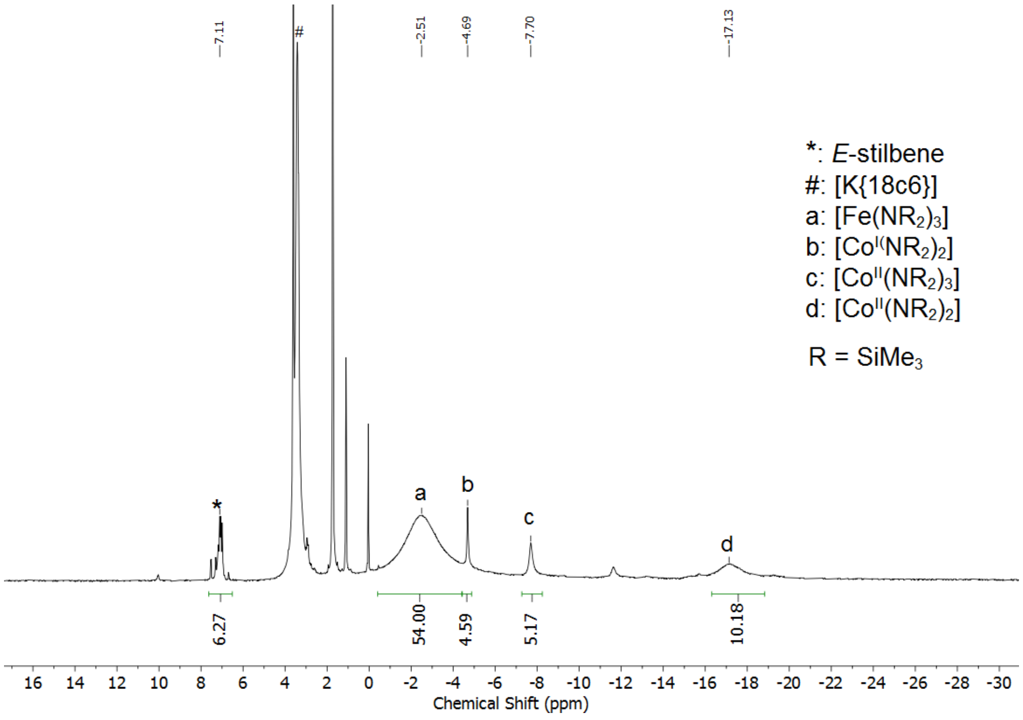

Figure S8. ^{1}H-NMR spectrum of the reaction of **1** with [Co^{II}(N(SiMe$_3$)$_2$)$_2$] in [D8]THF at 300 K, 300 MHz.

2.8. Attempted reaction of $[K\{18c6\}][Fe^{I}(N(SiMe_3)_2)_2]$ with *Z*-3-hexene

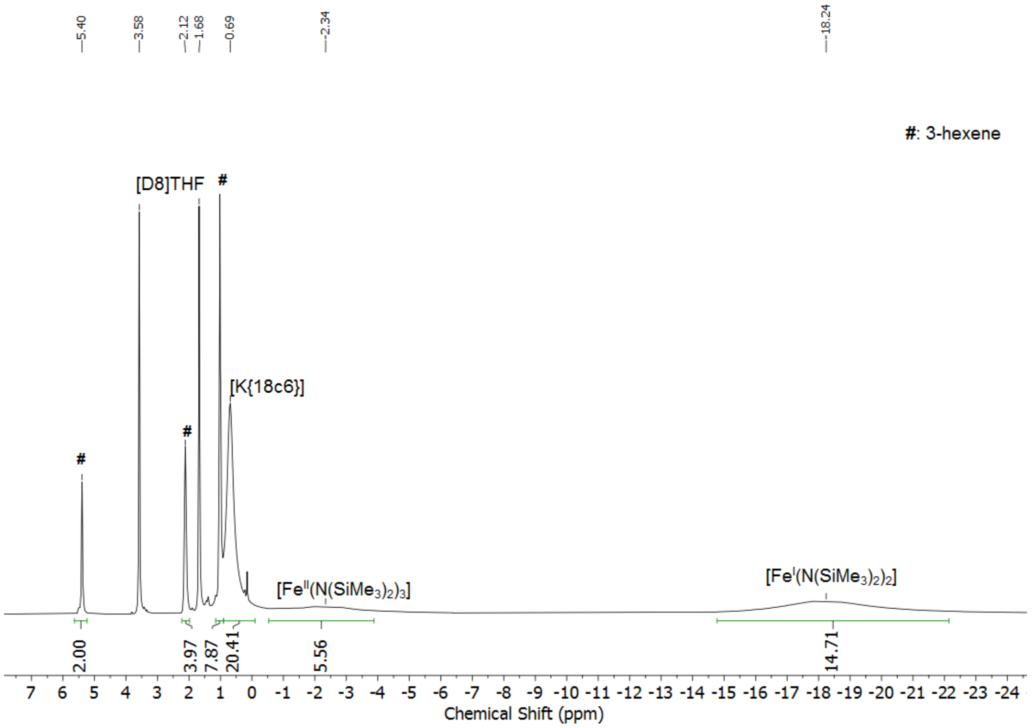

Figure S9. 1H-NMR spectrum of an equimolar mixture of $[K\{18c6\}][Fe^{I}(N(SiMe_3)_2)_2]$ with *Z*-3-hexene. Spectrum collected in [D8]THF at 300 K, 300 MHz. No signal for a hexene adduct with the iron(I) complex can be detected. **#**: 3-hexene (*E*/*Z*).

2.9. IR Spectroscopy

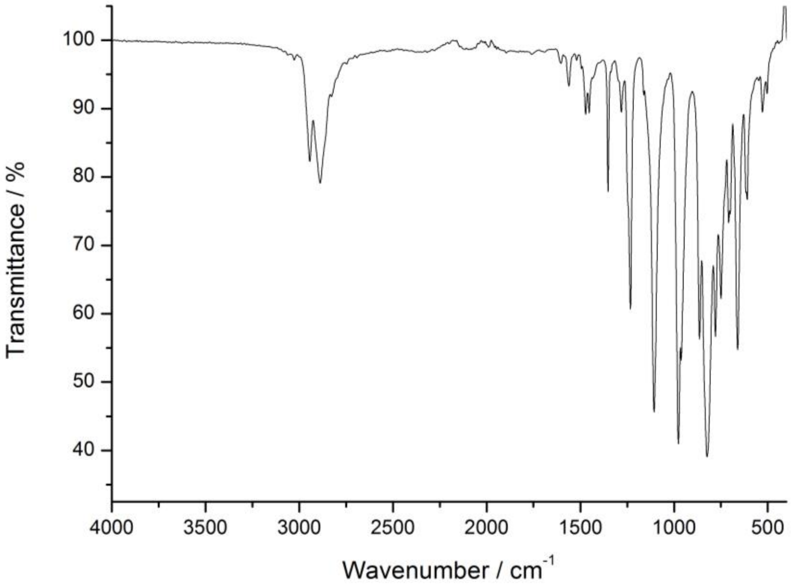

Figure S10. ATR-IR spectrum of **1**.

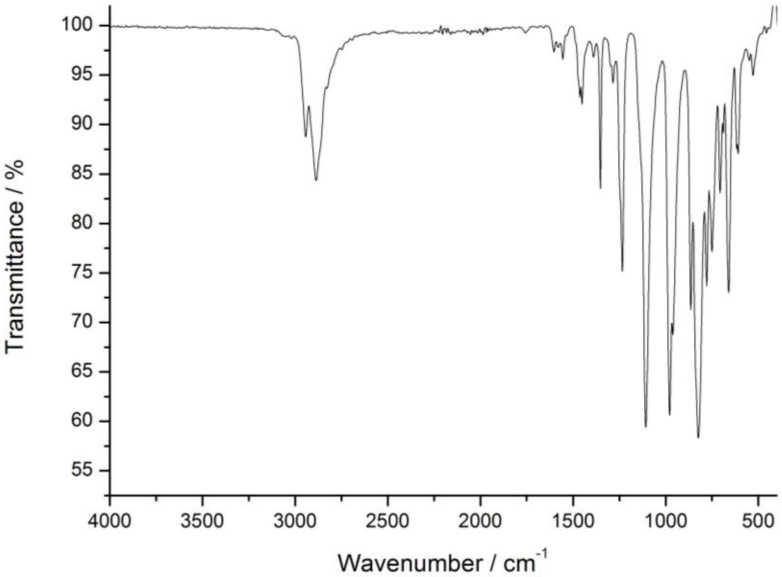

Figure S11. ATR-IR spectrum of **2**.

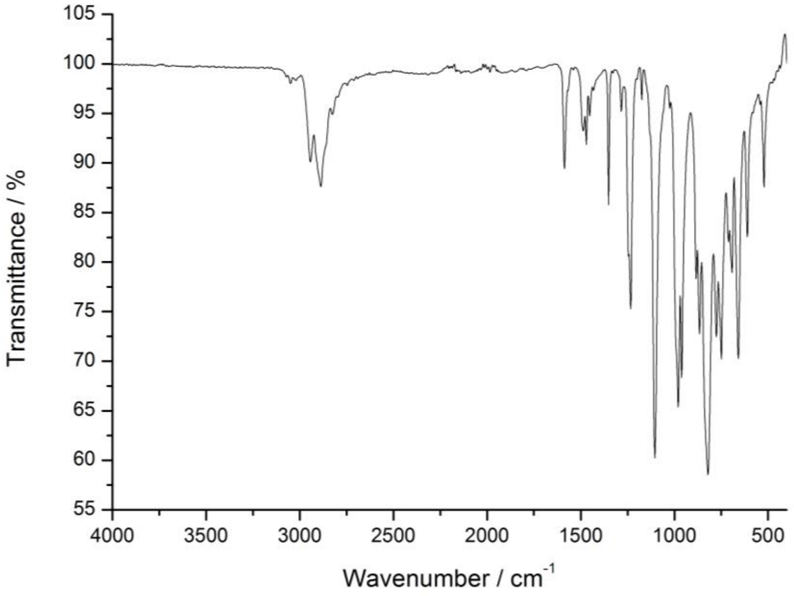

Figure S12. ATR-IR spectrum of **3**.

2.10. ^{57}Mössbauer spectroscopy

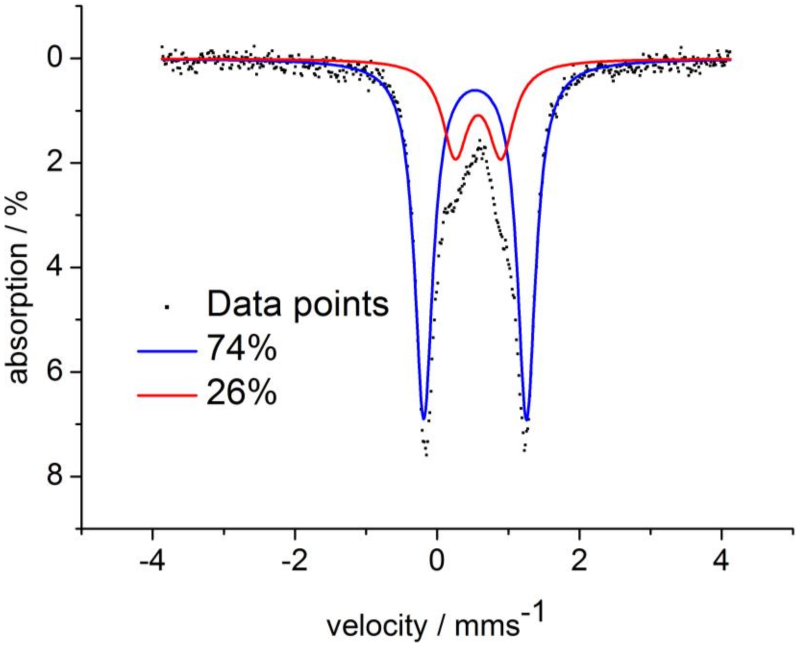

Figure S13. Zero-field ^{57}Mössbauer spectrum of **3** at 13 K. The blue line represents a fit with δ = 0.53 mms^{-1}, δQ = 1.44 mms^{-1} which can be assigned to **3** (74%). The red line represents a fit with δ = 0.57 mms^{-1}, δQ = 0.65 mms^{-1} which can be attributed to the decomposition product $[Fe(N(SiMe_3)_2)_3]^-$ (26%).[5]

2.11. EPR spectroscopy

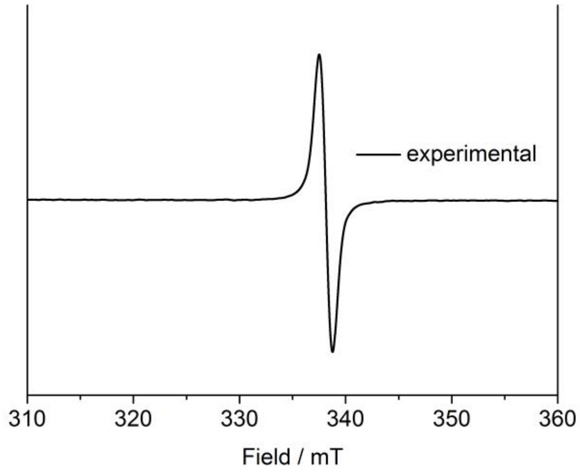

Figure S14. X-band EPR measurement of **3** in frozen toluene solution (9.476718 GHz) collected at 295 K. g = 2.002123.

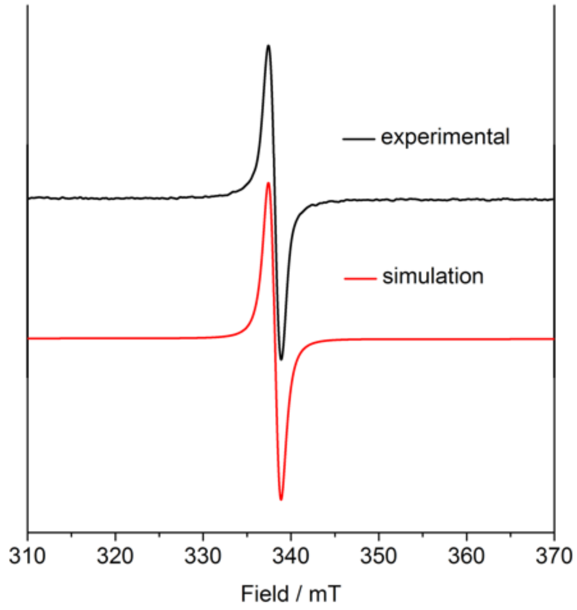

Figure S15. X-band EPR measurement of **1** in frozen toluene solution (9.476718 GHz) collected at 100 K (black) and simulated spectrum (red). g = 2.002396.

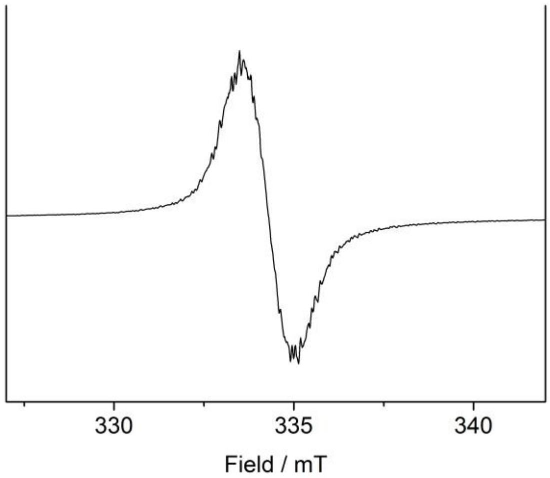

Figure S16. X-band EPR measurement of **3** in frozen toluene solution (9.368604 GHz) collected at 8 K. g = 2.004088.

2.12. UV Vis spectroscopy

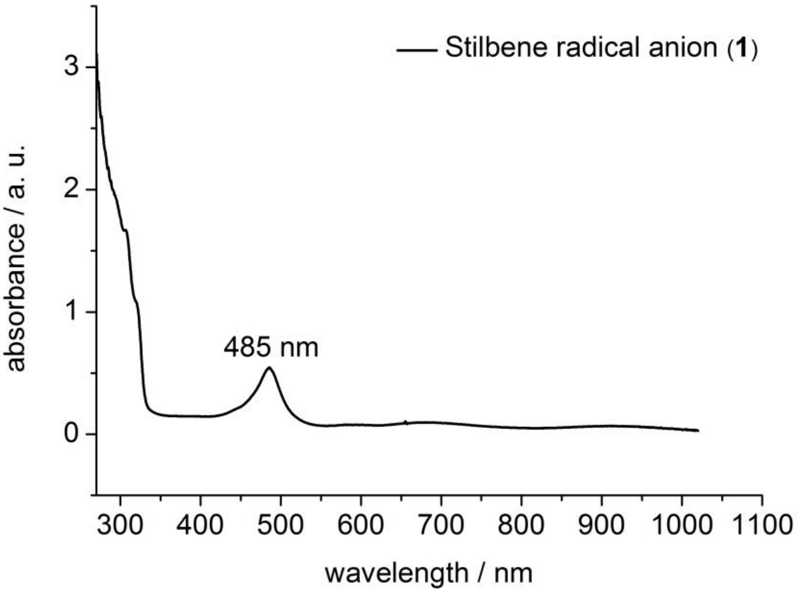

Figure S17. UV Vis spectrum of **1** in Et_2O at 300 K.

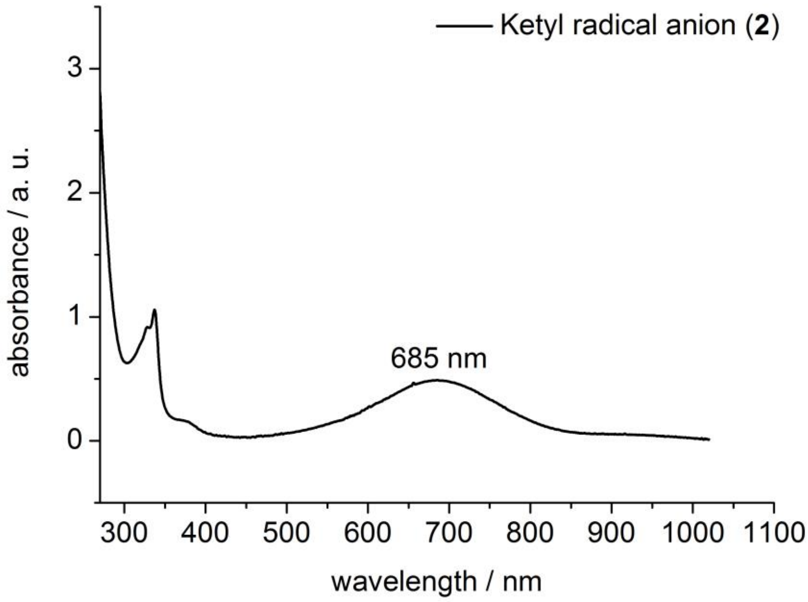

Figure S18. UV Vis spectrum of **2** in Et_2O at 300 K.

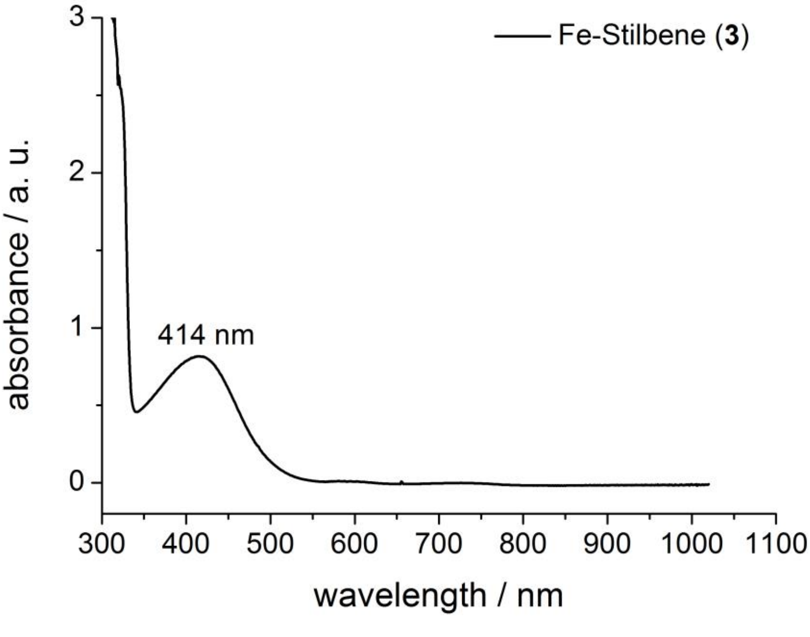

Figure S19. UV Vis spectrum of **3** in THF at 300 K.

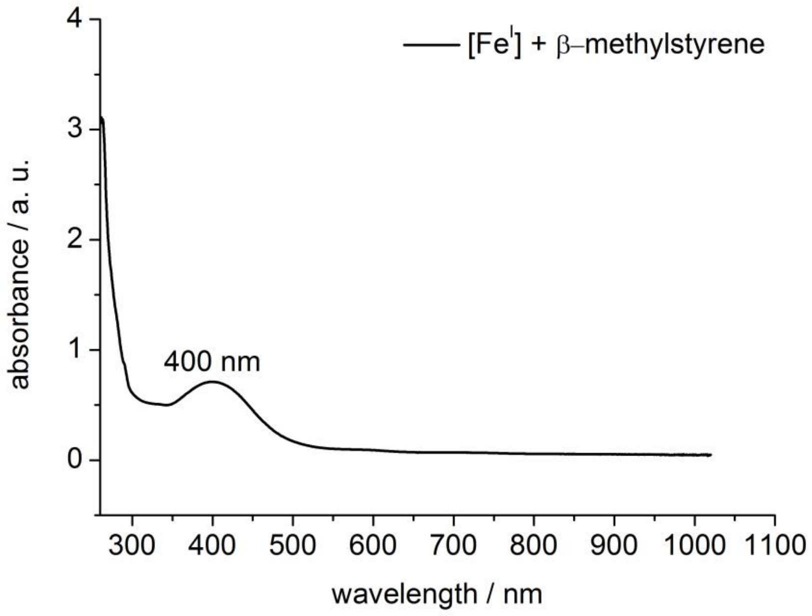

Figure S20. UV Vis spectrum of an equimolar mixture of [Fe^I] (= [K{18c6}][Fe(N(SiMe$_3$)$_2$)$_2$]) with ß-methylstyrene in Et$_2$O at 300 K.

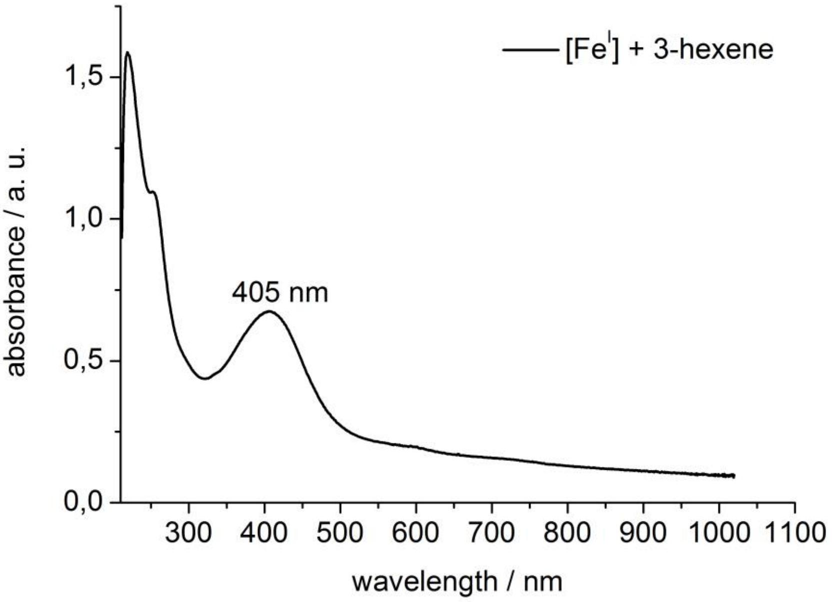

Figure S21. UV Vis spectrum of an equimolar mixture of [Fe^I] (= [K{18c6}][Fe(N(SiMe$_3$)$_2$)$_2$]) with 3-hexene in Et$_2$O at 300 K.

3. Catalysis

3.1. General procedure

The substrate and the catalyst were dissolved in [D8]THF under the exclusion of light. A fraction from the reaction mixture for the given reaction time was removed and quenched with a few drops of D_2O. The precipitate was filtered off and the filtrate was used as ^1H NMR sample. The conversion amount was determined as following:

$$conversion\% = \frac{\%E}{\%E + \%Z}$$

Relative amounts of *E* and *Z* isomers were determined via size of isomer-specific integrals in the ^1H NMR spectrum. An example of an ^1H NMR spectrum is given for each substrate.

3.2. Z to E isomerization of stilbene with KC_8 as catalyst

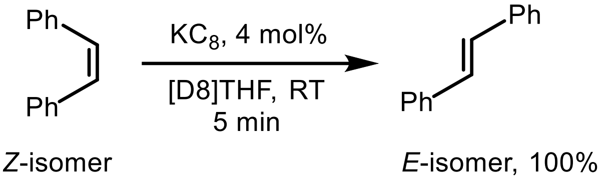

Scheme S1. Conversion of *Z*-stilbene into *E*-stilbene in [D8]THF using KC_8 as catalyst.

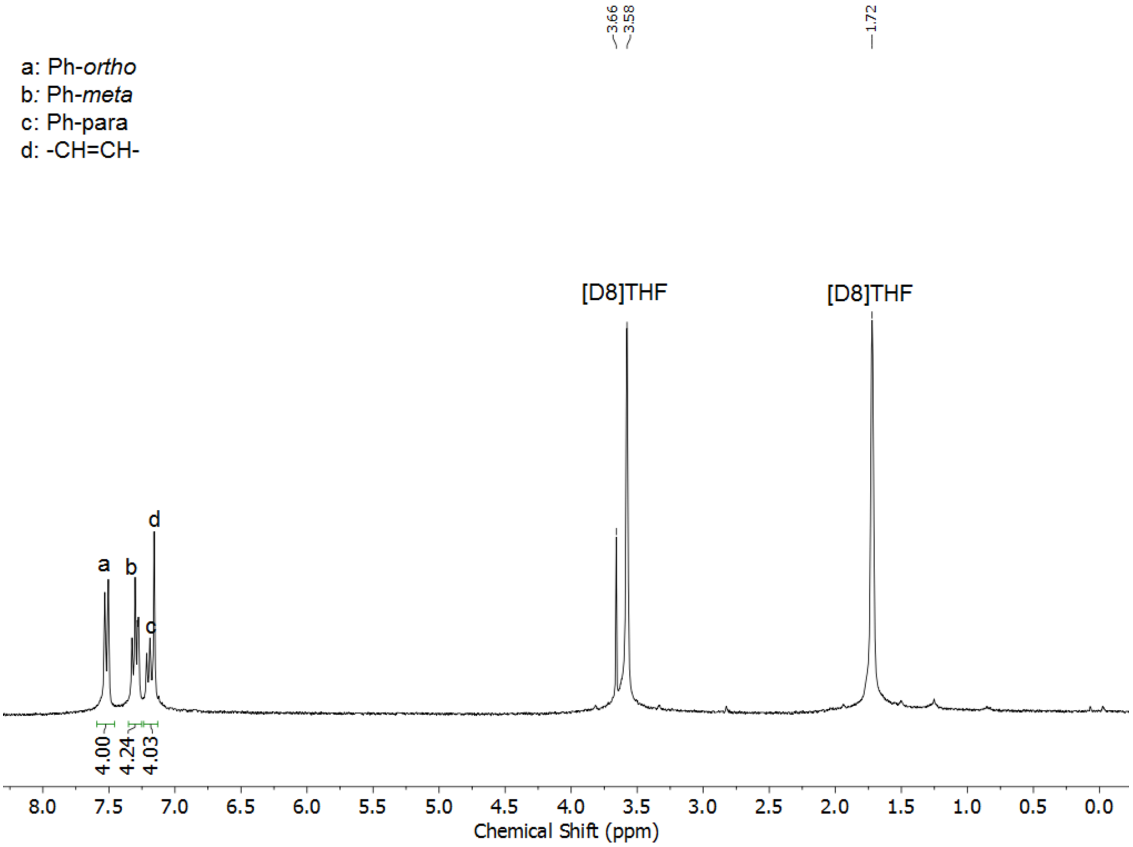

Figure S22. ^1H NMR spectrum of the conversion of Z-stilbene to E-stilbene in [D8]THF at 300K, 300 MHz using KC_8 as catalyst with 4 mol% catalyst load after 5 min. E isomer (100 %) can be detected. The spectrum was collected after quenching the reaction with D_2O.

3.3. Z to E isomerization of stilbene with 1 as catalyst

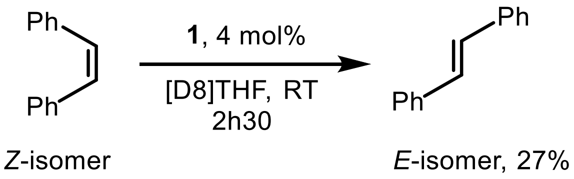

Scheme S2. Conversion of *Z*-stilbene into *E*-stilbene in [D8]THF using **1** as catalyst.

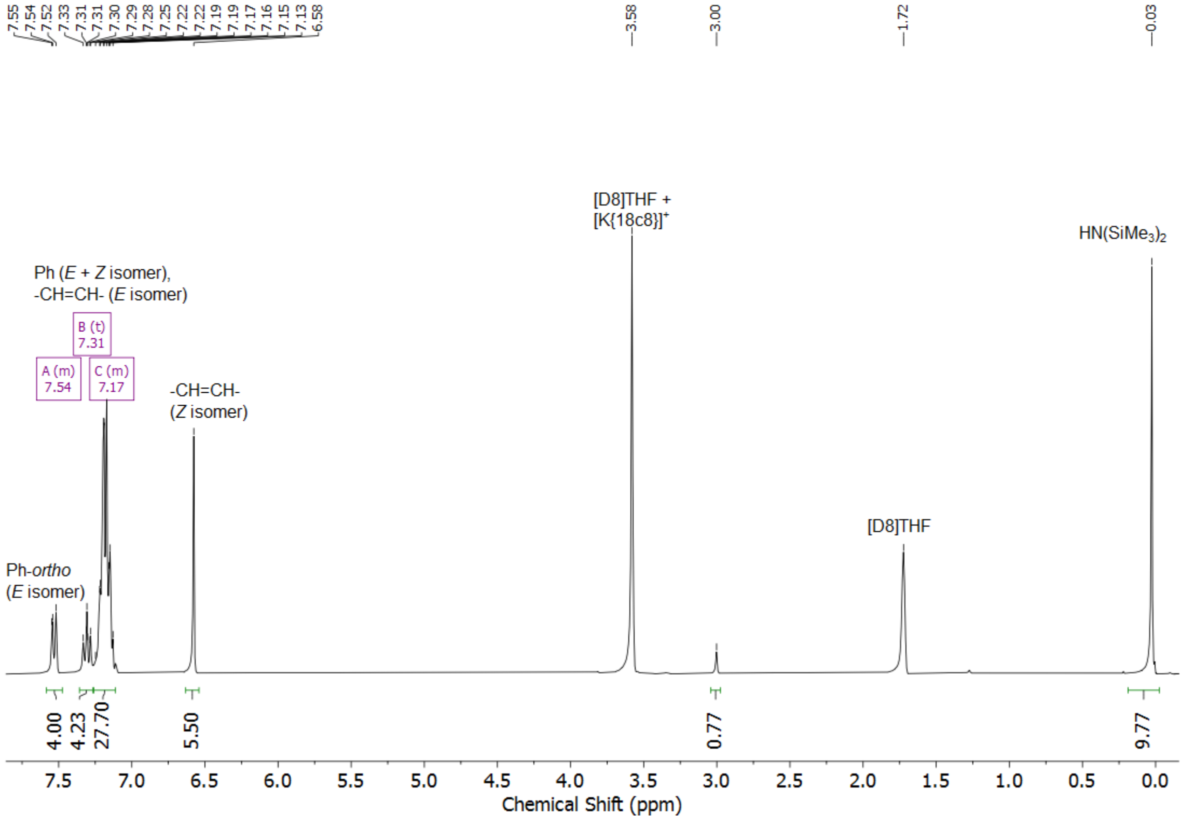

Figure S23. ^{1}H NMR spectrum of the conversion of Z-stilbene to E-stilbene in [D8]THF at 300K, 300 MHz using **1** as catalyst with 4 mol% catalyst load after 2h30. Z isomer (73 %) and E isomer (27 %) can be detected. The spectrum was collected after quenching the reaction with D_2O.

3.4. *Z* to *E* isomerization of stilbene with [K{18c6}][Fe^I(N(SiMe$_3$)$_2$)$_2$] as catalyst

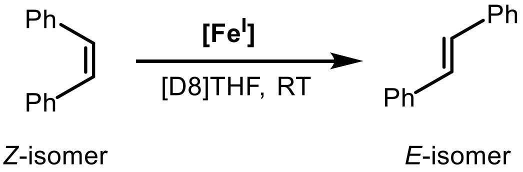

[Fe^I] = [K{18c$_6$}][Fe^I(N(SiMe$_3$)$_2$)$_2$]

Scheme S3. Conversion of Z-stilbene into E-stilbene in [D8]THF using [K{18c6}][Fe^I(N(SiMe$_3$)$_2$)$_2$] as catalyst.

Table S1. Conversion of Z-stilbene into E-stilbene in [D8]THF using [K{18c6}][Fe^{I}(N(SiMe$_3$)$_2$)$_2$] as catalyst.

cat. load	reaction time / min	conversion (%)
3mol%	5	51
3mol%	10	63
3mol%	15	71
3mol%	20	75
3mol%	30	83
3mol%	45	86
3mol%	60	90
3mol%	90	84
4mol%	5	47
4mol%	10	65
4mol%	15	76
4mol%	20	80
4mol%	25	85
4mol%	30	89
4mol%	45	95
4mol%	60	95
4mol%	90	100

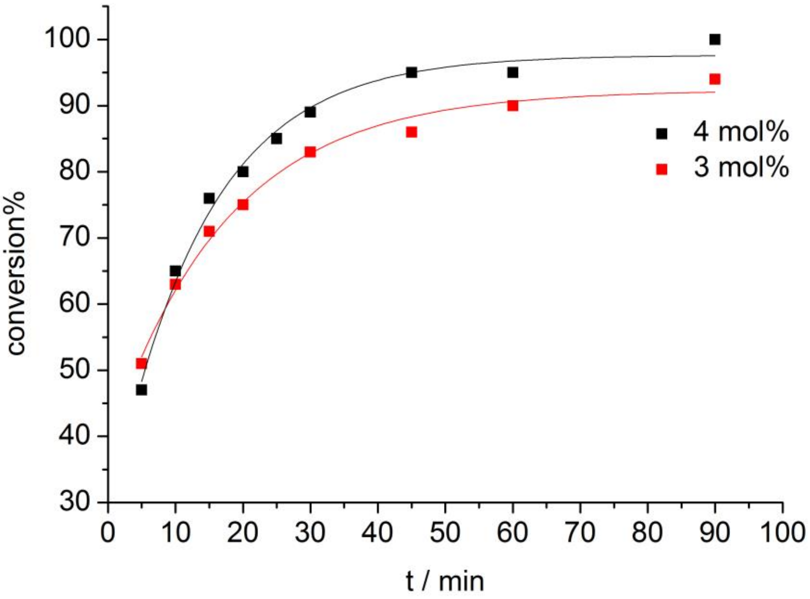

Figure S24. Conversion of Z-stilbene into E-stilbene in [D8]THF using [K{18c6}][Fe^{I}(N(SiMe$_3$)$_2$)$_2$] as catalyst with 3mol% catalyst load (red) and 4mol% catalyst load (black). Data points are represented as dots and the corresponding data fitting is represented as line.

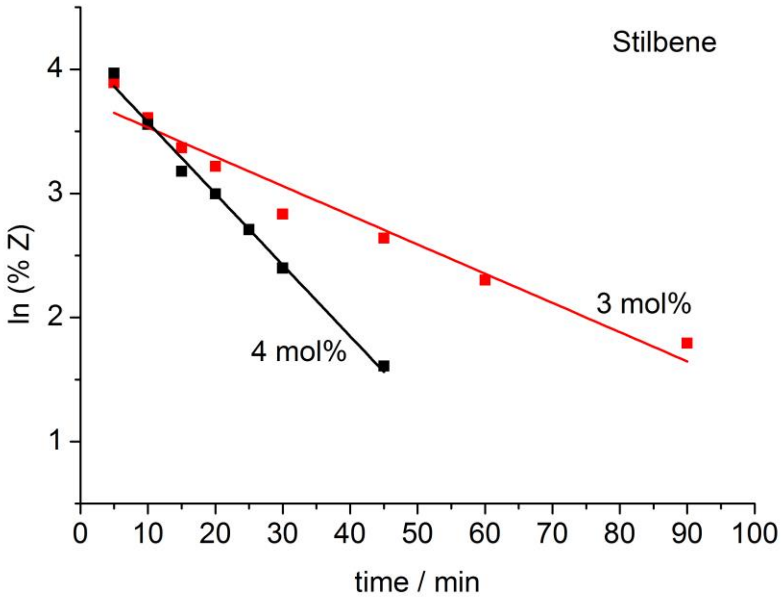

Figure S25. Conversion of Z-stilbene into E-stilbene in [D8]THF using [K{18c6}][Fe^I(N(SiMe$_3$)$_2$)$_2$] as catalyst with 3mol% catalyst load (red) and 4mol% catalyst load (black). Data points are represented as dots and the corresponding data fitting is represented as line. Logarithmic scale of %*Z*.

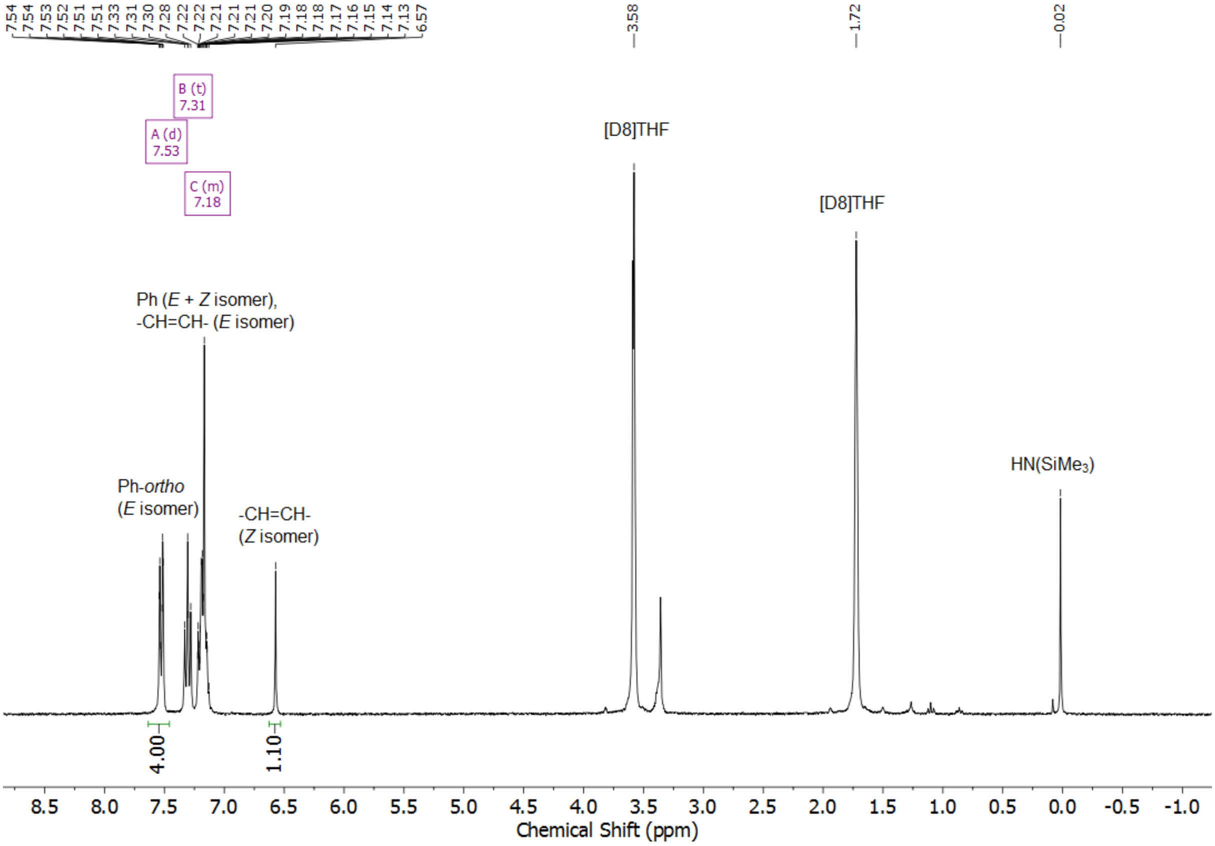

Figure S26. ^{1}H NMR spectrum of the conversion of *Z*-stilbene to *E*-stilbene in [D8]THF at 300K, 300 MHz using $[K\{18c6\}][Fe^I(N(SiMe_3)_2)_2]$ as catalyst with 10 mol% catalyst load after 10 min. *Z* isomer (35 %) and *E* isomer (65 %) can be detected. The spectrum was collected after quenching the reaction with D_2O.

3.5. *Z* to *E* isomerization of stilbene with [K{18c6}][Fe^I(N(Dipp)($SiMe_3$))$_2$] as catalyst

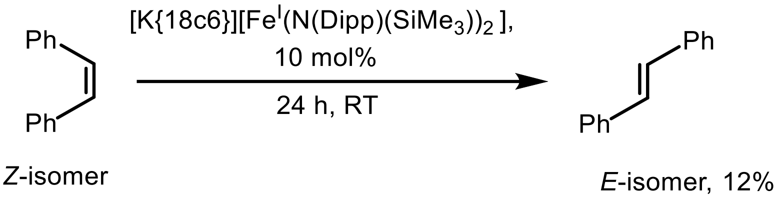

Scheme S4. Conversion of *Z*-stilbene into *E*-stilbene in [D8]THF using [K{18c6}][Fe^I(N(Dipp)($SiMe_3$))$_2$] as catalyst.

Table S2. Conversion of *Z*-stilbene into *E*-stilbene in [D8]THF using [K{18c6}][Fe^I(N(Dipp)($SiMe_3$))$_2$] as catalyst.

cat. load	reaction time	conversion (%)
10 mol%	3h45	5,4%
10 mol%	24h	12%

3.6. *Z* to *E* isomerization of ß-methylstyrene with [K{18c6}][Fe^I(N($SiMe_3$)$_2$)$_2$] as catalyst

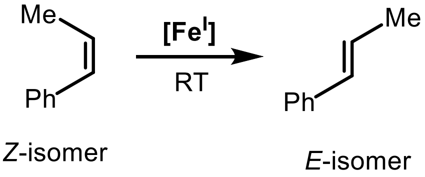

Scheme S5. Conversion of *Z*-ß-methylstyrene into *E*-ß-methylstyrene in [D8]THF using [K{18c6}][Fe^I(N($SiMe_3$)$_2$)$_2$] as catalyst.

Table S3. Conversion of *Z*-ß-methylstyrene into *E*-ß-methylstyrene in [D8]THF using [K{18c6}][Fe^I(N($SiMe_3$)$_2$)$_2$] as catalyst.

cat. load	reaction time / min	conversion (%)
10mol%	15	20
10mol%	30	26
10mol%	60	35
10mol%	90	43
10mol%	120	52
10mol%	194	62
10mol%	300	67

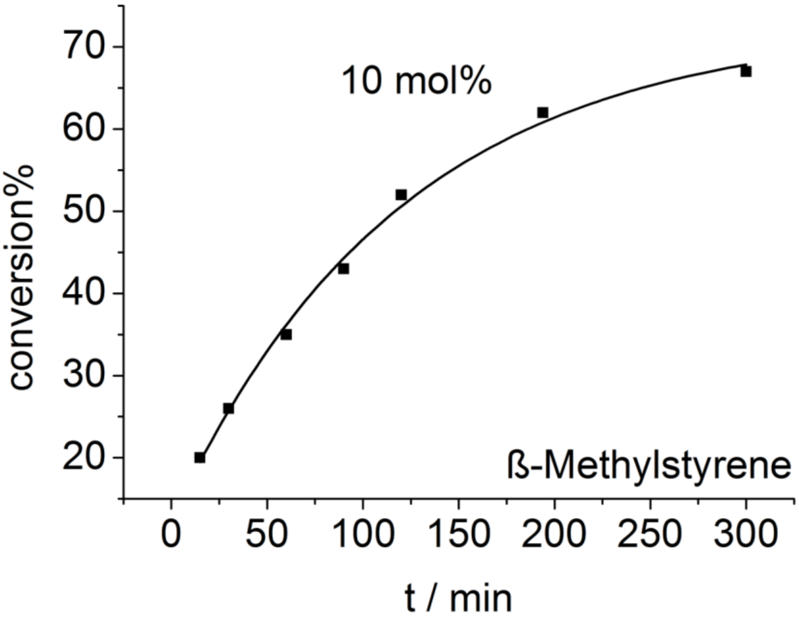

Figure S27. Conversion of *Z*-ß-methylstyrene into *E*-ß-methylstyrene in [D8]THF using [K{18c6}][Fe^{I}(N(SiMe$_3$)$_2$)$_2$] as catalyst with 10 mol% catalyst load. Data points are represented as dots and the corresponding data fitting is represented as line.

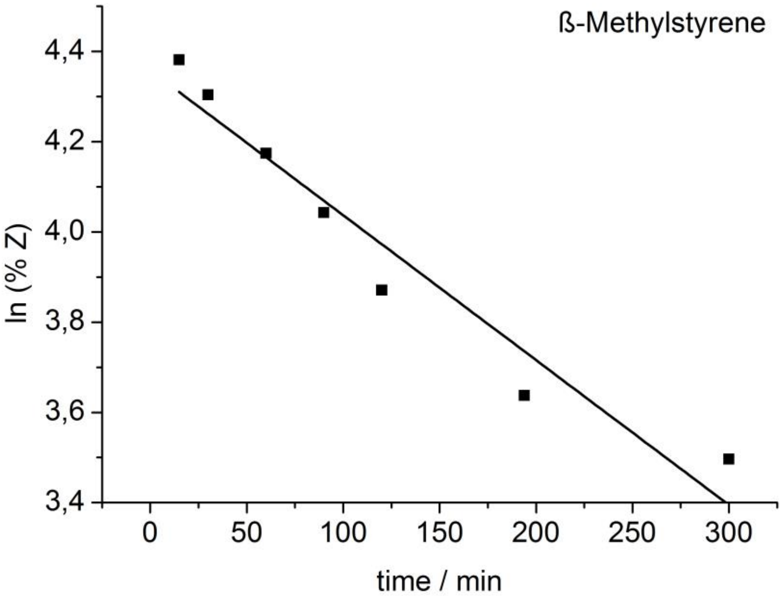

Figure S28. Conversion of *Z*-ß-methylstyrene into *E*-ß-methylstyrene in [D8]THF using [K{18c6}][Fe^{I}(N(SiMe$_3$)$_2$)$_2$] as catalyst with 10 mol% catalyst load. Data points are represented as dots and the corresponding data fitting is represented as line. Logarithmic scale of %*Z*

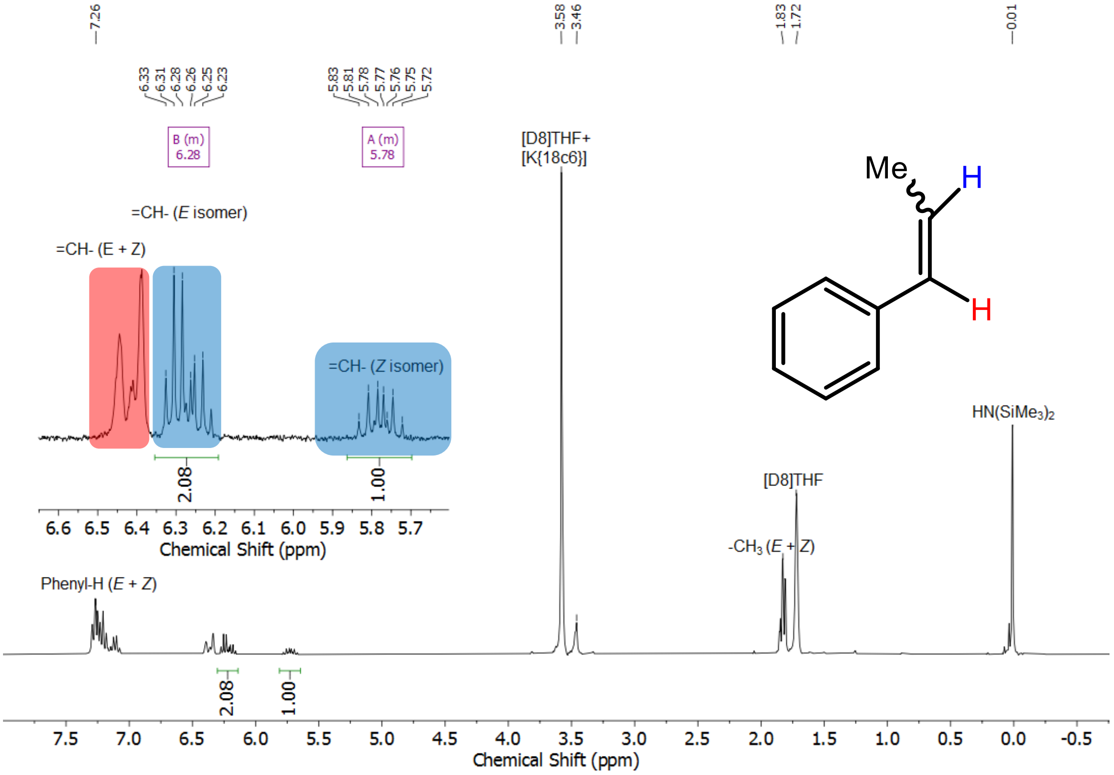

Figure S29. ^{1}H NMR spectrum of the conversion of *Z*-ß-methylstyrene to *E*-ß-methylstyrene in [D8]THF at 300 K, 300 MHz using [K{18c6}][Fe^I(N(SiMe$_3$)$_2$)$_2$] as catalyst with 10mol% catalyst load after 5 h. *Z* isomer (33 %) and *E* isomer (67 %) can be detected. The spectrum was collected after quenching the reaction with D_2O.

3.7. *Z* to *E* isomerization of 3-hexene with [K{18c6}][Fe^I(N(SiMe$_3$)$_2$)$_2$] as catalyst

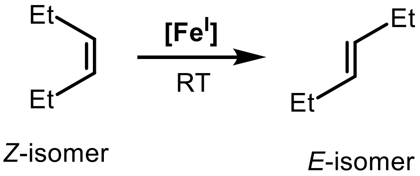

Scheme S6. Conversion of Z-3-hexene into E-3-hexene in [D8]THF using [K{18c6}][Fe^I(N(SiMe$_3$)$_2$)$_2$] as catalyst.

Table S4. Conversion of Z-3-hexene into E-3-hexene in [D8]THF using [K{18c6}][Fe^I(N(SiMe$_3$)$_2$)$_2$] as catalyst.

cat. load	reaction time	conversion (%)
10mol%	1 h	0
10mol%	1 d	25
10mol%	2 d	43
10mol%	3 d	58
10mol%	4 d	68
10mol%	7 d	75

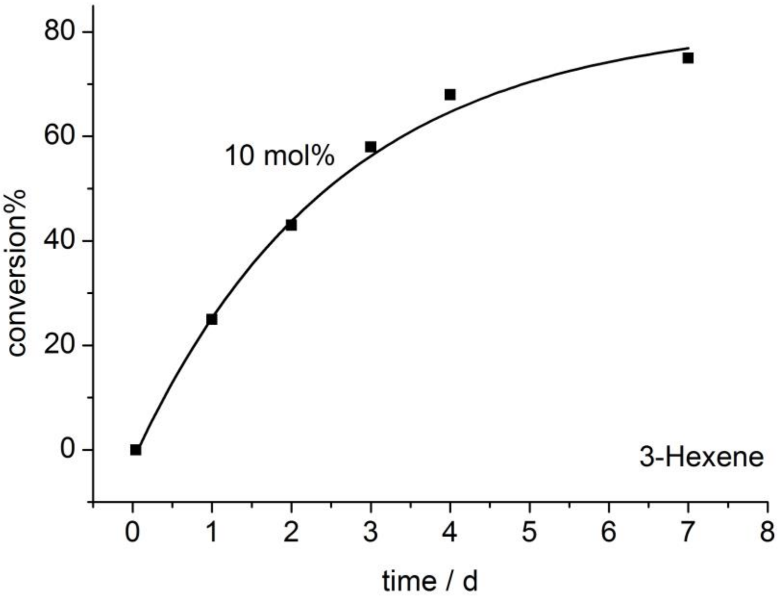

Figure S30. Conversion of *Z*-3-hexene into *E*-3-hexene in [D8]THF using [K{18c6}][Fe^I(N(SiMe$_3$)$_2$)$_2$] as catalyst with 10 mol% catalyst load. Data points are represented as dots and the corresponding data fitting is represented as line.

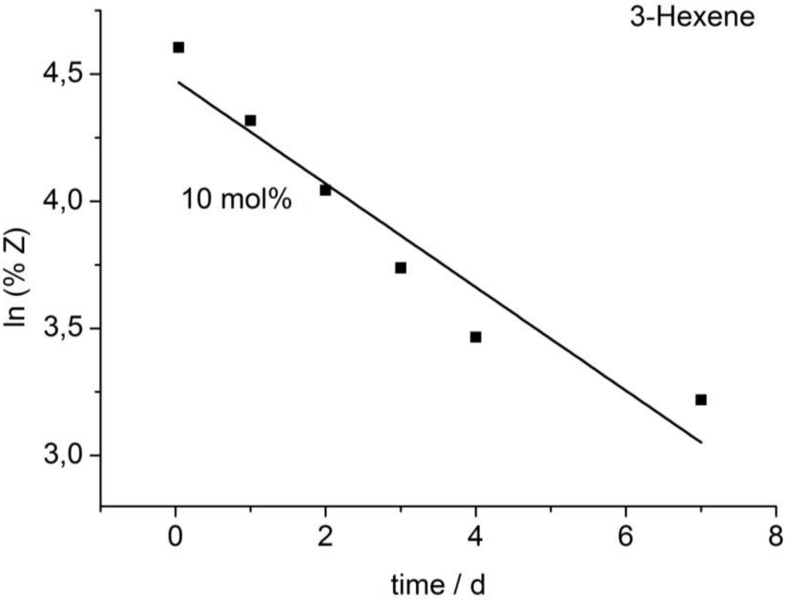

Figure S31. Conversion of *Z*-3-hexene into *E*-3-hexene in [D8]THF using [K{18c6}][Fe^I(N(SiMe$_3$)$_2$)$_2$] as catalyst with 10 mol% catalyst load. Data points are represented as dots and the corresponding data fitting is represented as line. Logarithmic scale of %*Z*.

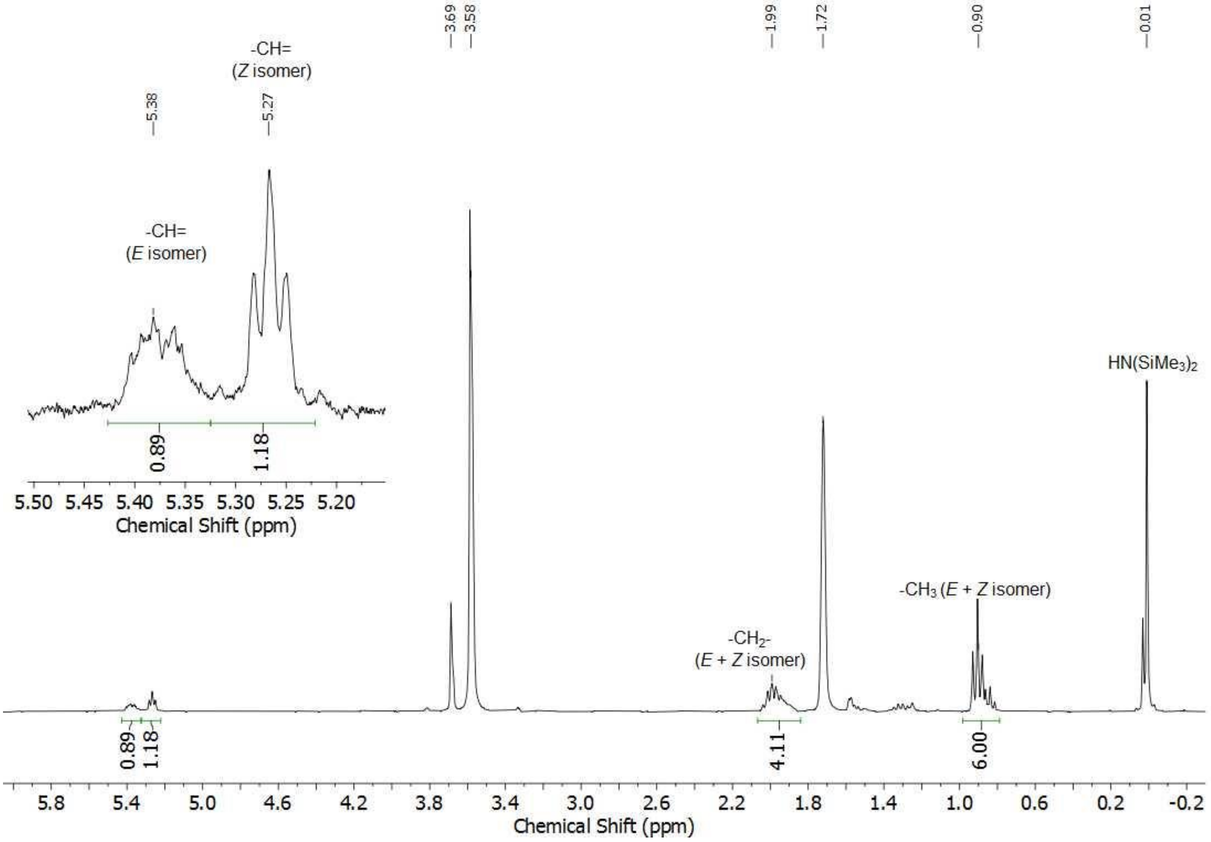

Figure S32. ^{1}H NMR spectrum of the conversion of *Z*-3-hexene to *E*-3-hexene in [D8]THF at 300 K, 300 MHz using [K{18c6}][$Fe^I(N(SiMe_3)_2)_2$] as catalyst with 10mol% catalyst load after 2 d. *Z* isomer (57 %) and *E* isomer (43 %) can be detected. The spectrum was collected after quenching the reaction with D_2O.

3.8. Poisoning experiment

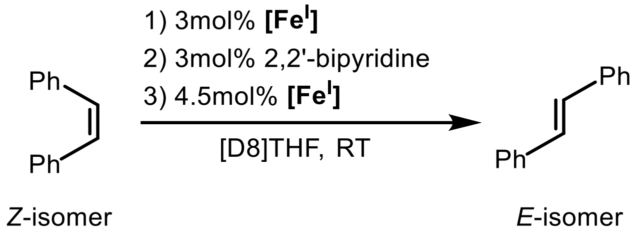

Scheme S7. Poisoning experiment for the isomerization of stilbene in [D8]THF with [Fe^I] as catalyst and 2,2'-bipyridine as poisoning reagent.

Table S5. Poisoning experiment for the isomerization of stilbene. 3mol% of 2,2'-bipyridine were added after 10 min to the initial mixture of Z-stilbene and 3mol% [**Fe**^{I}] in [D8]THF. 4.5mol% [**Fe**^{I}] were added after 40 min.

reaction time / min	conversion (%)
5	31
10	38
Addition of 3 mol% 2,2'bipyridine	
20	38
30	38
40	38.5
Addition of 4.5 mol% [**Fe**^{I}]	
50	73
60	87

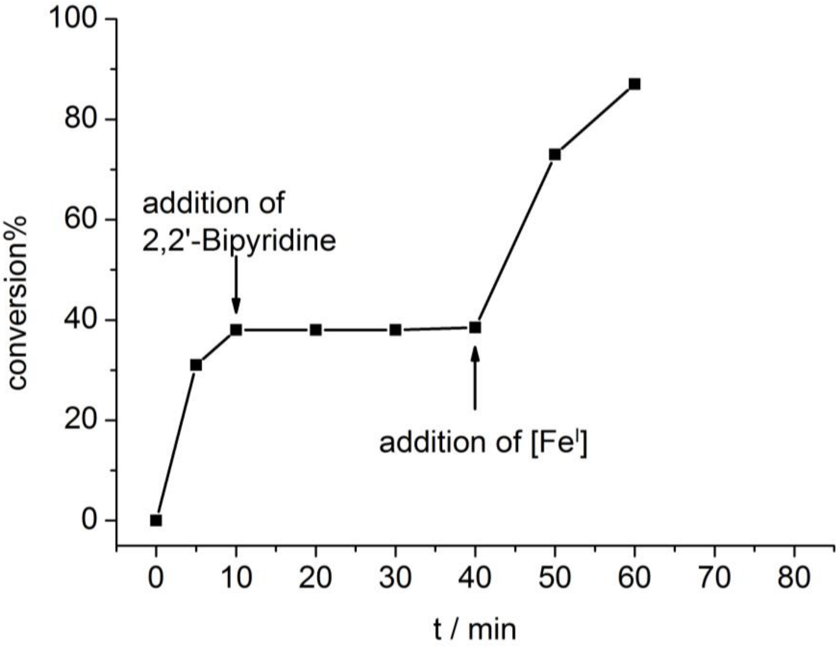

Figure S33. Poisoning experiment for the isomerization of stilbene. 3mol% of 2,2'-bipyridine were added to a mixture of Z-stilbene and 3mol% [**Fe**^{I}] in [D8]THF after 10 min. 4.5mol% [**Fe**^{I}] were added after 40 min.

4. Crystallography

Data for **1** (CCDC 2178650) and **2** (CCDC 2178649) were collected at 100 K on a BRUKER Quest D8 diffractometer using a graphite-monochromated Mo-Kα radiation and equipped with an Oxford Cryosystems Cryostream Coolder Device. Data for **3** (CCDC 2214046) and **4** (CCDC 2178651) were collected at 100 K on a STOE IPDS2 diffractometer, using a graphite-monochromated Mo-Kα radiation and equipped with an Oxford Cryosystems Cryostream Coolder Device. The structures have been solved using OLEX SHELXT V2014/1[6] and refinded by means of least-squares procedures on a F2 with the aid of the program SHELXL-2016/6, included in the software package WinGX version 1.63[7] or using CRYSTALS.[8] The Atomic Scattering Factors were taken from International Tables for X-Ray Crystallography.[9] All non-hydrogen atoms were refinded anisotropically. All hydrogen atoms were refinded by using a riding model. Absorption corrections were introduced by using the MULTISCAN[10] and X-Red program[11]. Drawings of molecules were performed with the program DIAMOND with 50% probability displacement ellipsoids for non-H atoms. H atoms are generally omitted for clarity.

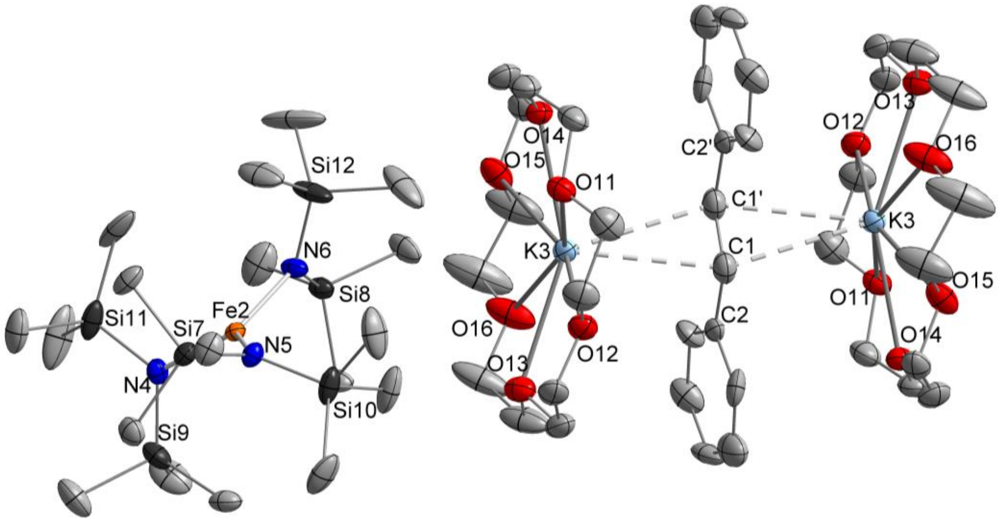

Figure S34. Molecular structure of **1**•(18c6)([K{18c6}][Fe(N(SiMe$_3$)$_2$)$_3$]) within the crystal. Hydrogen atoms, one molecule of [K(18c6)][Fe(N(SiMe$_3$)$_2$)$_3$] as well as one molecule of 18c6 have been omitted for clarity. Thermal ellipsoids are shown with 50% probability. An inversion-symmetrical disorder has been found for the stilbene fragment (50% / 50%).

Table S6. Crystal data and structure refinement of **1**•(18c6)([K{18c6}][Fe(N(SiMe$_3$)$_2$)$_3$]).

Identification code	**1**
Empirical formula	$C_{98}H_{216}Fe_2K_3N_6O_{24}Si_{12}$
Formula weight	2428.84
Temperature/K	100.0
Crystal system	monoclinic
Space group	*P*2$_1$/*n*
a/Å	16.0976(10)
b/Å	15.8981(8)
c/Å	26.7651(15)
α/°	90
β/°	93.037(2)
γ/°	90
Volume/Å^3	6840.1(7)
Z	2
ρ_{calc}g/cm^3	1.179
μ/mm^{-1}	0.468
F(000)	2630.0
Crystal size/mm^3	0.3 × 0.2 × 0.1
Radiation	MoKα (λ = 0.71073)
2Θ range for data collection/°	3.86 to 60.13
Index ranges	$-22 \le h \le 22$, $-22 \le k \le 22$, $-37 \le l \le 36$
Reflections collected	182148
Independent reflections	20029 [R_{int} = 0.0474, R_{sigma} = 0.0328]
Data/restraints/parameters	20029/149/889
Goodness-of-fit on F^2	1.026
Final R indexes [I>=2σ (I)]	R_1 = 0.0439, wR_2 = 0.1047
Final R indexes [all data]	R_1 = 0.0646, wR_2 = 0.1144
Largest diff. peak/hole / e Å^{-3}	0.67/-0.84

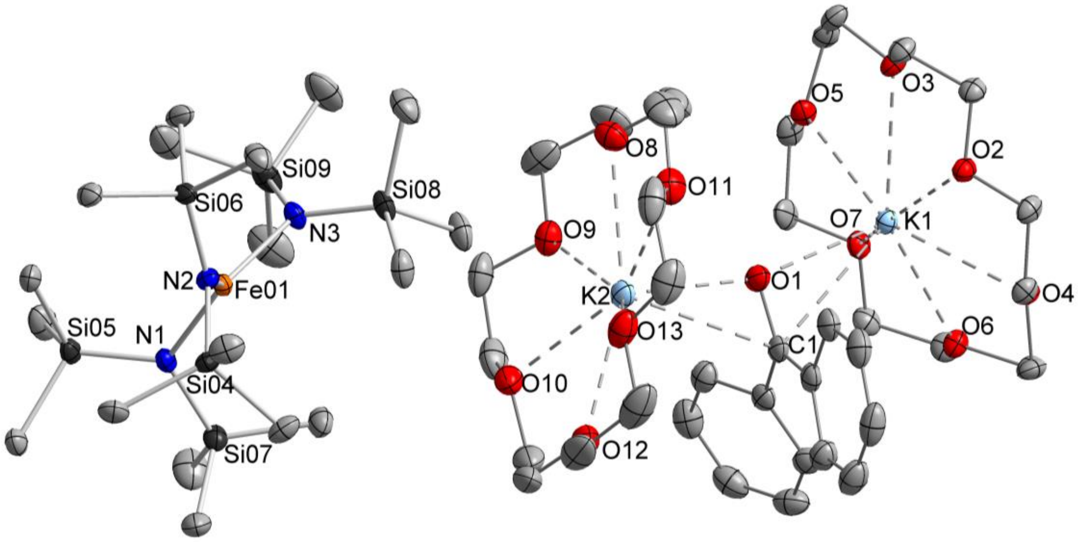

Figure S35. Molecular structure of **2** within the crystal. Hydrogen atoms are omitted for clarity, thermal ellipsoids are shown with 50% probability.

Table S7. Crystal data and structure refinement for **2**.

Identification code	**2**
Empirical formula	$C_{55}H_{112}FeK_2N_3O_{13}Si_6$
Formula weight	1326.06
Temperature/K	100.0
Crystal system	triclinic
Space group	P-1
a/Å	10.7165(3)
b/Å	17.9760(4)
c/Å	19.6298(4)
α/°	80.4780(10)
β/°	84.3760(10)
γ/°	84.0040(10)
Volume/Å^3	3696.40(15)
Z	2
ρ_{calc}g/cm^3	1.191
μ/mm^{-1}	0.467
F(000)	1430.0
Crystal size/mm^3	0.519 × 0.15 × 0.13
Radiation	MoKα (λ = 0.71073)
2Θ range for data collection/°	3.834 to 64.726
Index ranges	$-16 \le h \le 16$, $-26 \le k \le 27$, $-28 \le l \le 29$
Reflections collected	87985
Independent reflections	22101 [R_{int} = 0.0392, R_{sigma} = 0.0521]
Data/restraints/parameters	22101/60/902
Goodness-of-fit on F^2	1.075
Final R indexes [I>=2σ (I)]	R_1 = 0.0345, wR_2 = 0.0868
Final R indexes [all data]	R_1 = 0.0584, wR_2 = 0.0918
Largest diff. peak/hole / e Å^{-3}	0.66/-0.40

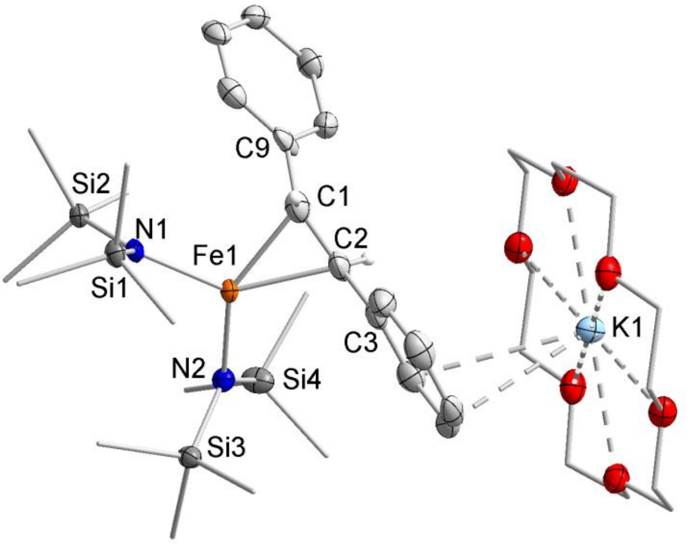

Figure S36. Molecular structure of **3**•0.5Et$_2$O within the crystal. Unnecessary hydrogen atoms and the co-crystallized Et$_2$O molecule are omitted for clarity. thermal ellipsoids are shown with 50 % probability. Et$_2$O is not depicted.

Table S8. Crystal data and structure refinment for **3**.

Identification code	**3**
Empirical formula	$C_{40}H_{77}FeKN_2O_{6.5}Si_4$
Formula weight	897.34
Temperature/K	100.00
Crystal system	monoclinic
Space group	C2/c
a/Å	37.3486(17)
b/Å	13.2014(4)
c/Å	27.113(2)
α/°	90
β/°	130.575(2)
γ/°	90
Volume/Å^3	10154.0(10)
Z	8
ρ_{calc}g/cm^3	1.174
μ/mm^{-1}	0.515
F(000)	3872.0
Crystal size/mm^3	0.731 × 0.101 × 0.028
Radiation	MoKα (λ = 0.71073)
2Θ range for data collection/°	3.956 to 51.996
Index ranges	$-46 \le h \le 46$, $-16 \le k \le 15$, $-33 \le l \le 33$
Reflections collected	145841
Independent reflections	9995 [R_{int} = 0.0878, R_{sigma} = 0.0386]
Data/restraints/parameters	9995/0/517
Goodness-of-fit on F^2	1.137
Final R indexes [I>=2σ (I)]	R_1 = 0.0549, wR_2 = 0.1045
Final R indexes [all data]	R_1 = 0.0710, wR_2 = 0.1086
Largest diff. peak/hole / e Å^{-3}	1.02/-0.36

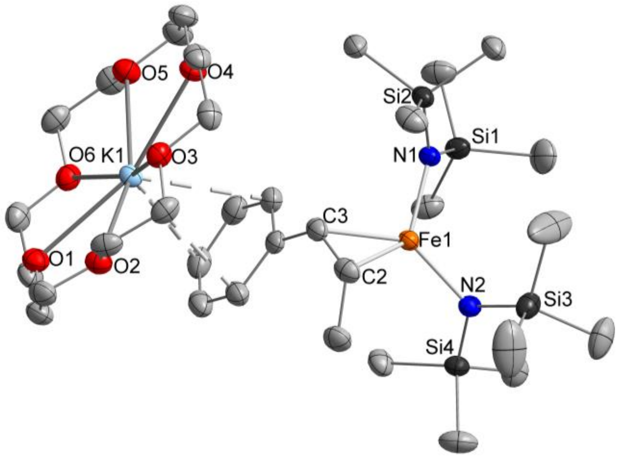

Figure S37. Molecular structure of **4** within the crystal. Hydrogen atoms are omitted for clarity, thermal ellipsoids are shown with 50% probability.

Table S9. Crystal data and structure refinement for **4**.

Identification code	**4**
Empirical formula	$C_{33}H_{70}FeKN_2O_6Si_4$
Formula weight	798.22
Temperature/K	100.0
Crystal system	monoclinic
Space group	$P2_1/c$
a/Å	12.1227(8)
b/Å	18.3502(12)
c/Å	21.0291(14)
α/°	90
β/°	104.641(5)
γ/°	90
Volume/Å^3	4526.1(5)
Z	4
ρ_{calc}g/cm^3	1.171
μ/mm^{-1}	0.569
F(000)	1724.0
Crystal size/mm^3	0.984 × 0.524 × 0.412
Radiation	MoKα (λ = 0.71073)
2Θ range for data collection/°	2.988 to 58.508
Index ranges	$-16 \le h \le 16$, $-22 \le k \le 25$, $-28 \le l \le 26$
Reflections collected	30974
Independent reflections	12149 [R_{int} = 0.0459, R_{sigma} = 0.0488]
Data/restraints/parameters	12149/0/437
Goodness-of-fit on F^2	0.951
Final R indexes [I>=2σ (I)]	R_1 = 0.0372, wR_2 = 0.0944
Final R indexes [all data]	R_1 = 0.0607, wR_2 = 0.1008
Largest diff. peak/hole / e Å^{-3}	0.74/-0.37

5. References

[1] S. Stoll, A. Schweiger, *J. Magn. Reson.* **2006**, *178*, 42–55.

[2] H. Bürger, U. Wannagat, *Monatsh. Chem.* **1963**, *94*, 1007–1012.

[3] C. G. Werncke, P. C. Bunting, C. Duhayon, J. R. Long, S. Bontemps, S. Sabo-Etienne, *Angew. Chem. Int. Ed.* **2015**, *54*, 245–248.

[4] C. G. Werncke, E. Suturina, P. C. Bunting, L. Vendier, J. R. Long, M. Atanasov, F. Neese, S. Sabo-Etienne, S. Bontemps, *Chem. Eur. J.* **2016**, *22*, 1668–1674.

[5] A. Eichhöfer, Y. Lan, V. Mereacre, T. Bodenstein, F. Weigend, *Inorg. Chem.* **2014**, *53*, 1962–1974.

[6] G. M. Sheldrick, *Acta Crystallogr., Sect. A: Found. Crystallogr.* **2015**, *71*, 3–8.

[7] L. Farrugia, *J. Appl. Crystallogr.* **1999**, *32*, 837.

[8] P. W. Betteridge, J. R. Carruthers, R. I. Cooper, K. Prout, D. J. Watkin, *J. Appl. Crystallogr.* **2003**, *36*, 1487.

[9] *International Tables for X-Ray Crystallography*, Kynoch Press, Birmingham, England, **1974**.

[10] *SADABS-2016/2*, Bruker, **2016**.

[11] *X-Area, X-Red 1.63.1.0*, STOE, **2016**.